Indian Journal of Pure & Applied Physics
Vol. 55, June 2017, pp. 420-430

Ab initio and DFT studies on structure, vibrational spectra of 4-tert-butyl-1,3-thiazol-2-amine (BTA)

V Vasantha Kumar[a], M Nagabhushanam[b] & J Laxmikanth Rao[c]*

[a]Department of Physics, Vignan Institute of Technology and Science, Hyderabad 500 007, India

[b]Department of Physics, University College of Science, Osmania University, Hyderabad 500 007, India

[c]I & PC Division, CSIR-Indian Institute of Chemical Technology, Hyderabad 500 007, India

Received 31 May 2016; revised 3 February 2017; accepted 27 February 2017

Theoretical studies have been carried out on 4-tert-butyl-1, 3-thiazol-2-amine (BTA) using both the B3LYP/6-311+G and HF/6-311+G methods. The geometrical parameters and vibrational spectra of BTA have been calculated and analyzed. The calculated IR wavenumbers have been compared with the observed FTIR wavenumbers. The complete assignments have been performed based on the potential energy distribution (PED) of the vibrational modes. The wavenumbers obtained from B3LYP method are in good agreement with the observed wavenumbers when compared to HF method. It has been found that there is an excellent correlation with 0.999 regression coefficient between the experiment and calculated vibrations. Thermal properties like rotational constants, zero point vibrational energies and nonlinear optical properties like dipole moment, hyperpolarizabilities, NBO analysis and the effect of temperature on various thermodynamic properties have been calculated and orted.

Keywords: Thiazole, FTIR spectra, DFT calculations, Hyperpolarizability, Thermodynamic properties

1 Introduction

Thiazoles that contain sulfur atom are the important class of heterocyclic compounds. These are present in many natural/synthetic products, which have a wide range of pharmacological activities[1,2] and also find various applications in the other fields such as polymers[3], liquid crystals[4], photonucleases[5], fluorescent dyes[6], insecticides[7] and antioxidant[8]. Some of the drugs that contain thiazole ring are anticonvulsant riluzole, antiparkinsonian talipexole, antischistosomal miridazole, antihelmintic tiabendazole, antiulcer alizatidine, vitamin B_1, antibacterial sulfathiazole, and antiviral ritonavir. In case of natural products thiazole is present as a subunit possessing different biological activities which play a vital role in the drug industry. Due to its fascinating biological activity, it is very interesting to study the geometrical, vibrational, thermal and nonlinear optical properties of the title molecule. Density functional theory (DFT) has become more useful to experimentalists in computing the geometrical parameters and other properties like vibrational, thermal, nonlinear, optical etc. of polyatomic molecules[9].

View metadata, citation and similar papers at core.ac.uk
brought to you by CORE
provided by Online Publishing @ NISCAIR

In the present study, the FTIR spectral investigations of BTA have been carried out theoretically using *ab initio* and DFT methods for the first time and the calculated vibrational wavenumbers are compared with the experiment. The title molecule considered for this study has been synthesized and reported by Kumar *et al.*[10] The geometrical parameters (like bond lengths, bond angles and dihedral angles), non-linear optical properties (like dipole moment, first hyperpolarizability and total hyperpolarizability), thermodynamic parameters (like total energy (E_{tot})), zero-point vibrational energy (*ZPVE*), heat capacities (C_v), entropy (S), total thermal energy (ε_{tot}), rotational temperatures (r_T) and HOMO-LUMO energy gap (ΔE_g) have been calculated and reported. The effect of temperature on some thermodynamic properties at various temperatures have been calculated and reported.

2 Computational Details

The geometry optimization of the molecule plays an important role in predicting the geometrical, thermal, spectral and NLO properties since these are controlled by the geometry of the molecule. Geometry optimizations of the title molecule, i.e., 4-tert-butyl-1,3-thiazol-2-amine (BTA) (Fig. 1) have been carried

*Corresponding author (E-mail: lkjoshiji@yahoo.com)

out with Gaussian 03W software[11] using HF/6-311+G and B3LYP/6-311+G methods. For selecting a suitable basis set for BTA, the calculations have been carried to evaluate the vibrational frequencies using different basis sets like 6-31G, 6-311G, 6-31G* and 6-311+G using both the HF and B3LYP methods[12,13]. Among all these basis sets, it is observed that the calculated vibrational frequencies using the 6-311+G basis set are in good agreement with the experimentally observed ones[10]. Also, to check the suitability of the basis set to explore properties of the BTA, calculations have been carried to evaluate the mean absolute deviation (MAD) values for the vibrational frequencies[12,13] using both HF and B3LYP methods. Here also it is observed that the MAD value calculated by 6-311+G basis set has shown less deviation when compared to the other basis sets. Hence, 6-311+G basis set has been chosen for further studies. During optimization, the atomic positions of the molecule have been fully relaxed and frequency calculations has been carried out to ensure that the optimized geometry that has all positive frequencies and thus is a minimum on the potential energy surface. In this study, it is observed that the vibrational wavenumbers calculated using the HF and B3LYP functional tend to overestimate the experimentally reported values; hence, wavenumbers of BTA are scaled to obtain correct values. In scaled quantum mechanical method, the systematic errors of the computed harmonic force field are corrected by a few scaling factors which are found to be well transferable between chemically related molecules[14-17] and these scaling factors are recommended for general use. In the scaling of vibrational frequencies of BTA, 0.855 (HF) and 0.92 (B3LYP) factors have been used for NH_2 functional group vibrations and remaining are scaled with 0.905 (HF) and 0.963 (B3LYP). The assignments of the calculated wavenumbers have been made by considering PEDs. The PEDs are computed for the quantum chemically calculated wavenumbers using VEDA 4 program[18] and Gauss View 3.0 package[19] have been used to get visual animation and also for the verification of the vibrational wavenumbers. The molecule belongs to Cs symmetry. The 60 vibrational modes of BTA are dispersed among the symmetry species as Γ = 36A' (in-plane) + 24A'' (out of plane). The calculated FTIR spectra of BTA using the B3LYP/6-311+G method is shown in Fig. 2 and for the sake of comparison the experimentally reported FTIR[10] spectra is also shown. The correlation plot between the calculated and experimental IR frequencies is shown in Fig. 3. It can be seen from Fig. 3 that the IR frequencies calculated using the B3LYP method are in good agreement with the experiment, when compared to the HF method, hence the spectral analysis has been discussed based on B3LYP/6-311+G results only. The optimized geometry obtained from both the HF and B3LYP methods has been used for calculating the thermodynamic and NLO properties of the title molecule. The effect of temperature on some thermodynamic parameters has been calculated and reported.

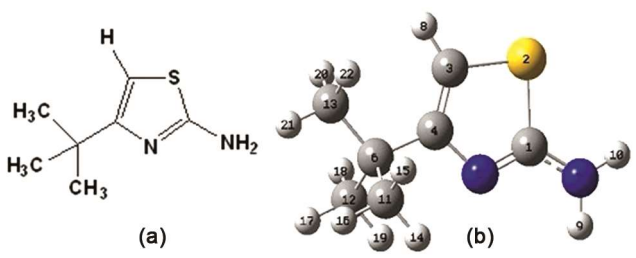

Fig. 1 — (a) Geometry of BTA and (b) optimized geometry of BTA with atom numbers

3 Geometric Structural Analyses

Since the molecular parameters are controlled by the molecular geometry, the geometry optimization is a crucial step for the calculation of IR spectra of BTA. The optimized bond lengths, bond angles and dihedral angles of BTA are given in Table 1, using both the methods namely HF/6-311+G and B3LYP/6-311+G methods. All bond lengths in thiazole ring are in the range of 1.85-1.30 Å, which are in good agreement with the reported data for thiazole[20] and methyl substituted amino thiazole[21]. The calculated bond length of -C_1N_7- in both the B3LYP (1.36 Å) and HF (1.35 Å) methods (Table 1) is in good agreement with the reported value of 1.34 Å for the substituted amino thiazole[21]. The calculated bond lengths of -C_1=N_5- and -C_3=C_4- are 1.30 and 1.36 Å, respectively, in B3LYP method, and 1.28 and 1.34 Å, respectively, in HF method (Table 1) which are in good agreement with the reported values 1.31 and 1.34 Å, respectively, for the substituted amino thiazole[21]. The calculated bond angles of -$S_2C_1N_5$-, -$S_2C_1N_7$- and -$N_5C_1N_7$- are 114.1°, 120.7° and 125.1°, respectively, in B3LYP method and 114.1°, 121.1° and 124.7°, respectively, in HF method (Table 1), which are in good agreement with the reported values of 115.0°, 121.0° and 123.5°, respectively, for the substituted amino thiazole[21].

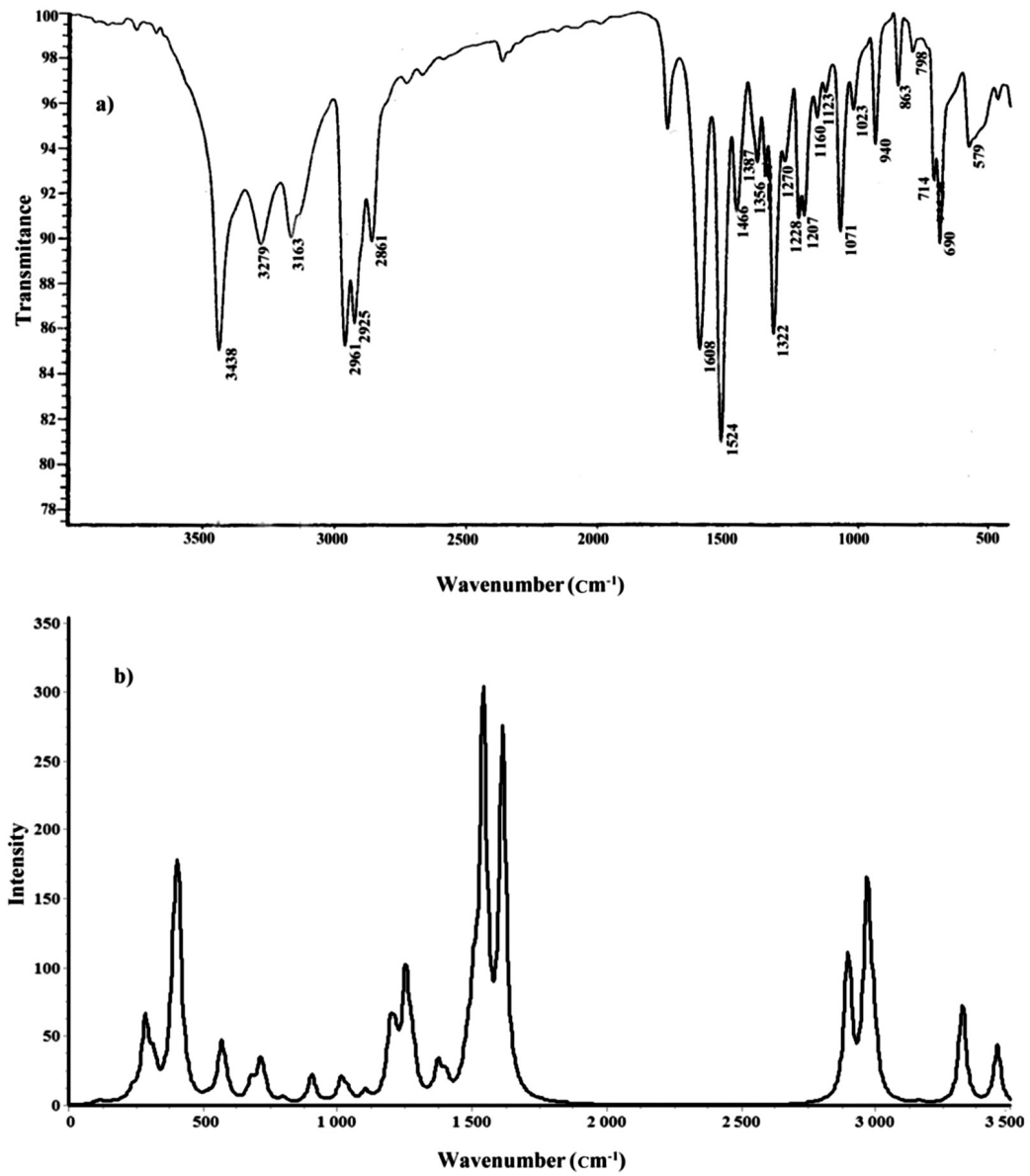

Fig. 2 — IR spectra of BTA (a) experimental FTIR spectra[10] in KBr and (b) calculated spectra obtained from B3LYP/6-311+G level theory (scaled)

4 Infrared Spectra Analysis

4.1 NH_2 vibrations

The IR frequencies corresponding to the symmetric and asymmetric stretching modes of amine functional group are very important in the primary amines moieties[21,22]. In all the primary aromatic amines, the ν-NH vibrational frequency[22,23] occurs in the region 3300–3500 cm^{-1}. Singh *et al.*[24], reported the symmetric and asymmetric stretching frequencies for the amino thiazole occurs at 3270 cm^{-1} and 3400 cm^{-1}, respectively. As the title molecule contains a primary amine group, the B3LYP calculated vibrational frequencies which occur at 3322 cm^{-1} and 3452 cm^{-1} have been assigned to the ν_s-NH and ν_{as}-NH vibrational frequencies, respectively (Fig. 2), which are in good agreement with the experimentally observed ν_s-NH (3279 cm^{-1}) and ν_{as}-NH (3438 cm^{-1}) frequencies, respectively[10]. As expected these two vibrational frequencies are pure stretching modes in nature and the respective PED contributions for symmetric and asymmetric stretching are 98% and 100%, respectively (mode numbers 1 and 2 in Table 2). Among the different vibrational modes of NH_2, the

scissoring mode has its own importance in IR spectrum while analyzing the spectrum of the molecule[23]. According to literature, the s-NH_2 mode[23,25] occurs in the region 1530-1650 cm^{-1}. In the case of amino thiazole, the s-NH_2 mode[24] is reported at 1620 cm^{-1} and Rao *et al.*[26] reported this modeat 1615 cm^{-1}. In the case of the title molecule, the s-NH_2 mode is observed at 1608 cm^{-1} and the calculated mode has been assigned at 1613 cm^{-1} (Fig. 2), which is in good agreement with both the reported and observed values[10]. The respective PED contribution for this mode is 86% (mode number 13) as shown in Table 2.

4.2 CH vibrations (ring)

The CH stretching vibrational mode in thiazoles and in substituted thiazoles[25,27] occurs in the region of 3190-3050 cm^{-1}. Sbrana *et al.*[28] reported this vibration at 3123 cm^{-1} in substituted thiazole. In the case of BTA, the observed value of ν–CH mode occurs at 3163 cm^{-1} and the calculated value has been assigned as 3162 cm^{-1} with its corresponding PED as 99% (mode number 3). In substituted amino thiazoles, the β-CH mode[25] occurs in the region of 1077-1140 cm^{-1}. In the case of BTA the calculated value for β-CH mode is 1102 cm^{-1} which is in good agreement with both the observed (1123 cm^{-1}) and the reported values[10,25,28] and the PED contribution for this mode is 63% (mode number 30) (Table 2).

According to literature the experimental γ-CH vibrational modes in substituted thiazoles[25] occur in the region 650-700 cm^{-1} and this mode has been observed for BTA at 690 cm^{-1}, which is in good agreement with the calculated value of 677 cm^{-1} and the PED contributions for this mode are 93% and 76% (mode number 41 and 40, respectively) (Table 2).

4.3 CH_3 vibrations

In case of stretching vibrations, which are characteristic for the CH_3 group and the two significant bands which arise due to the asymmetrical

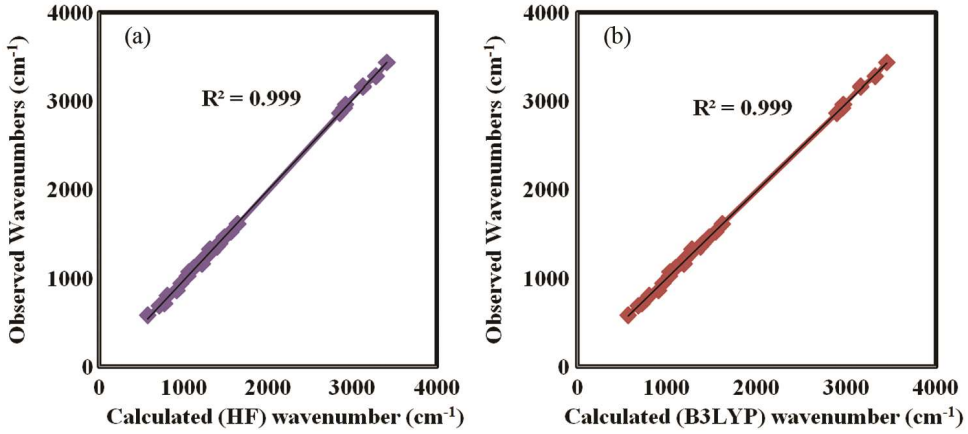

Fig. 3 — Correlation plot of IR frequencies between (a) HF/6-311+G Vs experimental frequencies (Y_{HF} = 1.020X + 46.3) and (b) B3LYP/6-311+G Vs experimental frequencies of BTA (Y_{B3LYP} = 0.988X +13.63)

Table 1 — Calculated bond lengths, bond angles and dihedral angles for BTA at HF/6-311+G and B3LYP/6-311+G methods

Bond length (Å)			Bond angle (°)			Dihedral angle (°)		
	HF	B3LYP		HF	B3LYP		HF	B3LYP
C_1S_2	1.81	1.85	$C_1S_2C_3$	86.63	86.06	$N_7C_1S_2C_3$	-180.0	180.0
C_1N_5	1.28	1.30	$C_1N_5C_4$	113.39	113.16	$N_7C_1N_5C_4$	180.0	-180.0
C_1N_7	1.35	1.36	$C_3C_4N_5$	115.28	115.42	$S_2C_3C_4C_6$	-180.0	179.9
C_3S_2	1.81	1.82	$C_3C_4C_6$	127.57	127.07	$C_1N_5C_4C_6$	-180.0	-180.0
C_3C_4	1.34	1.36	$N_5C_4C_6$	117.14	117.51	$C_3C_4C_6C_{11}$	-120.4	-120.4
N_5C_4	1.40	1.41	$C4C_6C_{11}$	108.70	108.78	$C_3C_4C_6C_{12}$	120.4	120.5
C_4C_6	1.52	1.52	$C_4C_6C_{12}$	108.70	108.78	$N_5C_4C_6C_{11}$	59.6	59.5
C_6C_{11}	1.54	1.55	$C_4C_6C_{13}$	111.24	111.22	$N_5C_4C_6C_{12}$	-59.6	-59.5
C_6C_{12}	1.54	1.55	$C_{11}C_6C_{12}$	109.54	109.37	$N_5C_4C_6C_{13}$	180.0	-179.9
C_6C_{13}	1.54	1.54	$C_{11}C_6C_{13}$	109.32	109.34			
			$C_{12}C_6C_{13}$	109.32	109.33			
			$S_2C_1N_5$	114.10	114.10			
			$S_2C_1N_7$	121.10	120.70			
			$N_5C_1N_7$	124.70	125.10			

Table 2 — Calculated and observed infrared wavenumbers (cm^{-1}) and assignments with potential energy distribution (PED) of BTA

Mode No	Species	Calculated wavenumber				Observed wavenumber	Assignment (%PED)
		HF/6-311+G		B3LYP/6-311+G			
		Unscaled	Scaled	Unscaled	Scaled		
1	A'	3991	3412	3753	3452	3438	νasNH(100)
2	A'	3841	3284	3611	3322	3279	νsNH(98)
3	A'	3457	3129	3284	3162	3163	νC2H4(99)
4	A'	3254	2945	3108	2992		νCH3-dia(93)
5	A"	3249	2940	3103	2988		νCH3-dia(93)
6	A'	3223	2917	3084	2969	2961	νCH3-dia(98)
7	A"	3220	2914	3081	2967		νCH3(96)
8	A'	3211	2906	3075	2961		νCH3-dia(96)
9	A"	3207	2903	3073	2958	2925	νCH3-dia(95)
10	A'	3158	2858	3014	2902		νCH3-sym(96)
11	A'	3148	2849	3006	2894		νCH3-sym(96)
12	A"	3148	2849	3006	2894	2861	νCH3-sym(96)
13	A'	1813	1641	1675	1613	1608	s NH2(86)+νC1N20(12)
14	A'	1722	1559	1601	1541		ν NCN(84)+ s NH2(15)
15	A'	1714	1551	1565	1506	1524	δCH3-dia(41)+ νC6C2(33)
16	A'	1669	1510	1548	1490		δCH3-dia(38)+ ν C6C2(43)
17	A"	1655	1498	1542	1485		δCH3-dia(60)
18	A'	1648	1491	1533	1476		δCH3-dia(83)
19	A"	1642	1486	1527	1470		δCH3-dia(87)
20	A'	1641	1486	1527	1470	1466	δCH3-dia(86)
21	A"	1627	1473	1512	1456		δCH3-dia(90)
22	A'	1576	1426	1455	1401	1387	δCH3-sym(79)
23	A'	1548	1401	1429	1375		δCH3-sym(86)
24	A"	1544	1398	1423	1370	1356	δCH3-sym(97)
25	A'	1452	1314	1327	1277		νNC(34)+rCH3(25)+ rNH2(28)
26	A'	1428	1292	1300	1252		rNH2(68)+νN20C1(13)+ βC2H4(14)
27	A'	1372	1242	1260	1213		rCH3(52)+βC2H4(35)
28	A'	1352	1224	1241	1194		ν C7C16(26) + rCH3(35)
29	A"	1348	1220	1237	1191		r CH3(73)
30	A'	1244	1126	1145	1102	1123	βC2H4(63)+rNH2(21)
31	A'	1173	1062	1077	1036		rCH3(52)+βC2H4(15)
32	A"	1159	1049	1067	1027		rCH3(62)
33	A'	1144	1035	1052	1012		r CH3(35)+r NH2(11)
34	A"	1070	969	990	953		rCH3(68)
35	A'	1027	929	952	916		r CH3(78)
36	A'	1021	924	939	904		ν C7C8(35)+r CH3(52)
37	A"	1015	919	938	903		βC2C6N5(30)+rCH3(21)
38	A'	888	804	827	796		ν C6C7(15)+rCH3(32)
39	A'	855	774	750	722		ν S3C2(75)
40	A"	801	725	738	710		γ C2H4(76)

(Contd.)

Table 2 — Calculated and observed infrared wavenumbers (cm^{-1}) and assignments with potential energy distribution (PED) of BTA *(Contd.—)*

Mode No	Species	Calculated wavenumber				Observed wavenumber	Assignment (%PED)
		HF/6-311+G		B3LYP/6-311+G			
		Unscaled	Scaled	Unscaled	Scaled		
41	A"	787	712	704	677	690	γ C2H4(93)
42	A'	682	618	609	586		ν S3C1(24)+rNH2(46)
43	A"	665	602	589	567		τS3C1N5(61)+ζ NH2(35)
44	A'	635	575	585	563		δCH3(30)+νS3N5(24)+ r NH2(46)
45	A'	582	526	539	519		ν C6C7(32)+γC1S3C2(15)
46	A'	501	453	463	446		s C12C8(35)+s C6C16(23)
47	A"	486	440	424	407		ω NH2(81)
48	A"	439	398	407	392		ω NH2(50)+ rCH3(48)
49	A'	401	363	370	356		bendNH2(45)+ bend CH3(35)
50	A"	371	336	327	314		bendCH3(30)+ γ N20H22(70)
51	A'	347	314	313	301		bendNH2(11)+ bendCH3 (27)
52	A'	336	304	307	295		δ CCC(46)
53	A"	329	298	297	285		τ CH3(78)
54	A"	321	291	295	283		τ NH2(70)
55	A'	293	265	267	257		τ CH3(63)
56	A"	269	244	245	236		τ C2C6N5(30)+τ N5C1N20(60)
57	A"	247	224	225	216		τ CH3(81)
58	A'	191	173	176	169		β CH3(35)+ β NH2(61)
59	A"	131	119	119	114		β CH3(30)+ γ C6N5(63)
60	A"	59	54	49	47		δ CH3(50)+ ζ* (45)

and symmetrical stretching vibrations occurs in the region of 3000-2850 cm^{-1}, respectively[12,13,22]. The reported values for these vibrational modes are 2960 cm^{-1}, 2935 cm^{-1} (asymmetrical) and 2860 cm^{-1} (symmetrical)[28]. In the title molecule, the calculated values for the above mentioned vibrations appears at 2894 cm^{-1} (symmetric) and 2969 and 2958 cm^{-1} (asymmetric), which are in good agreement with the observed values, i.e., 2861 cm^{-1} (symmetric) and 2961 and 2925 cm^{-1} (asymmetric)[10]. The PED contribution for these vibrations is ~ 96% (mode numbers 6, 9 and 12) (Table 2).

In case of methyl substituted amino thiazoles, the methyl deformation vibrations occur in the region of 1350-1475 cm^{-1}. The reported values for the symmetric and asymmetric deformation vibrations are 1460 cm^{-1} and 1375 cm^{-1}, respectively[25]. In case of BTA, the calculated values for the methyl deformation vibrations appear at 1470 cm^{-1} (asymmetric) and 1401 cm^{-1} and 1370 cm^{-1} (symmetric), which are in good agreement with the observed vibrations that occurs at 1466 cm^{-1} for asymmetric and 1387 cm^{-1} and 1356 cm^{-1} for symmetrical modes[10]. The PED contributions of these modes have been mentioned in Table 2 (mode numbers 15 to 24).

4.4 C=N, C-N, S-C vibrations (ring)

In general, the -C=N- ring stretching vibrational mode[23,25] occurs in the range 1550-1505 cm^{-1}. In case of BTA, the calculated value of 1541 cm^{-1} for this vibration mode is in good agreement with both the observed (1524 cm^{-1}) and the reported values. In thiazole ring, the reported values for the -C-N- ring stretching vibrations[24,28] are 1322 cm^{-1} and 1315 cm^{-1}. In case of BTA, the calculated -C-N- vibration occurs at 1277cm^{-1}, which is in good agreement with the observed (1322 cm^{-1}) and reported values. In amino thiazole, the reported value for -S-C- vibrational mode[23] is 690 cm^{-1}. In case of BTA, the calculated -S-C- vibration occurs at 722 cm^{-1}, which is in good agreement with both the observed (714 cm^{-1}) and the reported values[23]. The corresponding PEDs have been mentioned in Table 2 (mode 25 to 39).

5 Natural Bond Orbital (NBO) Analyses

NBO analysis provides an efficient method for studying the intra and intermolecular bonding and the interaction among bonds and also useful for investigating the charge transfer or conjugative interaction in molecular systems[29]. This can be done by considering all possible interactions between filled

donor and empty acceptor NBOs and estimating their energy by second order perturbation theory. For each donor NBO (i) and acceptor NBO (j) the stabilization energy $E(2)$ associated with electron delocalization between donor and acceptor is estimated as:

$$E(2) = \Delta E_{\mathrm{ij}} = q_{\mathrm{i}}\left(\frac{F(i,j)^2}{(E_{\mathrm{j}} - E_{\mathrm{i}})}\right) \quad \ldots (1)$$

where q_{i} is the orbital occupancy, E_{j} and E_{i} are diagonal elements and $F(i, j)$ is the off-diagonal NBO Fock matrix element. The larger $E(2)$ value indicates the more intensive interaction between electron donors and electron acceptors, i.e., more donating tendency from electron donors to electron acceptors and greater is the extent of conjugation in the whole system.

In the present study, NBO analysis has been performed on the title molecule at the DFT/B3LYP/6-311+G level and the results of the second order perturbation theory analysis of Fock matrix are shown in Table 3. The strong intra-molecular hyper conjugative interaction of the σ and π electrons of (C−C), (C−N) and (C−S) to the anti σ and π electrons of (C−C), (C−N) and (C−S) bonds leads to stabilization of the ring system. The interaction of σ (C_1-N_5) to σ*(C_6-C_7) leads to stabilization of ~ 3.0 kcal/mole and the interactions between σ (C_2-S_3) to σ*(C_1-N_{20}) and σ*(C_6-C_7) result in the stabilization of 3.9 and 6.3 kcal/mole, respectively. The interaction of σ (N_5-C_6) to σ*(C_1-N_{20}) and σ (C_7-C_{16}) to σ*(N_5-C_6) leads to stabilization of approximately 6.7 and 3.8 kcal/mole, respectively. The most important interactions related to the resonance in the molecule are electron donation from the lone pairs of S_3, N_5 and N_{20} to the bonding and antibonding orbitals. The interactions between the LP(2) S_3 of the ring hetero atom to the anti bonding orbitals namely π*(C_1-N_5) and π*(C_2-C_6) result in the stabilization of 20.32 and 12.86 kcal/mole, respectively. The interactions between the LP(1) N_5 of the ring hetero atom to the anti bonding orbitals namely π*(C_1-N_5) and π*(C_2-C_6) results having the stabilization of 20.32 and 12.86 kcal/mole, respectively, which indicates the delocalization. The interaction between the π*(C_1-N_5) to π*(C_2-C_6) results in the stabilization of ~ 42 kcal/mol. The interaction between LP(1) N20 with the π*(C_1-N_5) results in the stabilization of ~ 50 kcal/mol denotes larger delocalization within the ring.

Table 3 — Second order perturbation energy (E(2), kcal/mol) between donor and acceptor orbitals of BTA calculated at B3LYP/6-311+G method

Donor (i)	Acceptor (j)	$E(2)$[a]	$E(j)$-$E(i)$[b] (au)	$F(i,j)$[c] (au)
σ (C_1-S_3)	σ *(C_2 - H_4)	2.01	2.01	0.042
	σ *(N_{20}-H_{21})	2.55	1.07	0.047
σ (C_1- N_5)	σ *(C_6- C_7)	2.69	1.29	0.053
π(C_1 - N_5)	π *(C_2 - C_6)	18.67	0.35	0.075
σ (C_2 - S_3)	σ *(C_1- N_{20})	3.88	1.05	0.057
	σ *(C_6- C_7)	6.24	1.01	0.071
σ (C_2 – H_4)	σ *(C_2 - C_6)	2.82	1.17	0.051
	σ *(N_5 - C_6)	4.47	1.00	0.060
σ (C_2 - C_6)	σ *(C_2 - H_4)	2.07	1.25	0.045
	σ *(C_6- C_7)	3.14	1.16	0.054
π (C_2 - C_6)	π *(C_1- N_5)	7.55	0.27	0.044
	π *(C_7 - C_8)	2.16	0.64	0.034
	π *(C_7 - C_{12})	2.16	0.64	0.034
σ (N_5 - C_6)	σ *(C_1- N_{20})	6.56	1.21	0.080
	σ *(C_2 - H_4)	2.32	1.25	0.048
σ (C_6 - C_7)	σ *(C_2 - S_3)	2.79	0.77	0.042
σ (C_7 - C_8)	π * (C_2 - C_6)	2.49	0.61	0.037
σ (C_7 - C_{12})	σ * (C_2 - C_6)	2.49	0.61	0.037
σ (C_7 - C_{16})	σ *(N_5 - C_6)	3.75	1.03	0.055
σ (C_8 - H_9)	σ *(C_7 - C_{16})	2.92	0.86	0.045
σ (C_8 – H_{10})	σ * (C_7 - C_{12})	2.87	0.85	0.044
σ (C_8 – H_{11})	σ *(C_6- C_7)	2.78	0.90	0.045
σ (C_{12} - H_{13})	σ *(C_6- C_7)	2.79	0.90	0.045
σ (C_{12} - H_{14})	σ *(C_7 - C_8)	2.87	0.85	0.044
σ (C_{12} - H_{15})	σ *(C_7 - C_{16})	2.92	0.86	0.045
σ (C_{12} - H_{17})	σ *(C_7 - C_8)	2.91	0.86	0.045
σ (C_{12} - H_{18})	σ *(C_6- C_7)	3.10	0.91	0.048
σ (C_{12} - H_{19})	σ * (C_7 - C_{12})	2.91	0.86	0.045
σ (N_{20}- H_{21})	σ *(C_1 - S_3)	5.14	0.81	0.059
	σ *(C_1 - N_5)	4.85	1.27	0.070
LP(1)S_3	σ *(C_1 - N_5)	2.35	1.25	0.048
LP(2)S_3	π *(C_1 - N_5)	20.32	0.25	0.066
	π *(C_2 - C_6)	12.86	0.29	0.054
LP(1)N_5	σ *(C_1 - S_3)	18.92	0.47	0.085
	σ *(C_1 - N_{20})	2.47	0.81	0.041
	σ *(C_2 - C_6)	5.94	0.97	0.069
LP(1) N_{20}	π *(C_1 - N_5)	49.81	0.27	0.109
π * (C_1-S_3)	π *(C_1 - S_3)	41.92	0.04	0.063

For numbering of atoms of BTA refer Fig. 1; [a] Energy of hyper conjugative interactions; [b] Energy difference between donor and acceptor i and j NBO orbitals; [c] Fock matrix element between i and j NBO orbitals

6 Thermodynamic Properties

The study of thermodynamic properties of organic molecules has its own importance in the research area. The thermodynamic properties like total energy (E_{tot}), zero-point vibrational energy (ZPVE), heat capacities (C_{v}), entropy (S), total thermal energy (ϵ_{tot}), rotational constants (r_{C}) and rotational temperatures (r_{T}) of BTA have been calculated at constant pressure using the B3LYP/6-311+G and HF/6-311+G optimized geometries and the results are given in Table 4. It can

be seen from the Table 4, that the variation in E_{tot} and ZPVEs obtained for the title molecule using both the B3LYP/6-311+G and HF/6-311+G methods are significant. The E_{tot} values obtained for BTA using B3LYP/6-311+G and HF/6-311+G methods are -781.65 and -953.81 au, respectively. The ZPVEs values obtained for BTA using B3LYP/6-311+G and HF/6-311+G methods are 115.34 and 123.418 kcal/mol, respectively. The rotational constant values are observed to be nearly same in both the methods. Dipole moment reflects the molecular charge distribution in the molecule and is given as a vector in three dimensions. Therefore, it can be used to depict the charge movement across the molecule. The dipole moment values calculated using both the methods differ slightly.

Table 4 — Thermodynamic parameters of BTA

	HF/6-311+G	B3LYP/6-311+G
Thermal parameters		
E_{tot}	-953.81	-781.65 hartrees
ZPVE	123.418	115.34 Kcal/mol
r_c	2.12050	2.08048 GHz
	0.76354	0.75169
	0.64047	0.62931
r_T	0.10177	0.09985 Kelvin
	0.03664	0.03608
	0.03074	0.03020
Thermal energy (Є) (Kcal/mol)		
$Є_{trans}$	0.889	0.889
$Є_{rot}$	0.889	0.889
$Є_{vib}$	128.101	120.556
$Є_{tot}$	129.878	122.334
Specific heat (C_v) (Cal/mol-K)		
C_{trans}	2.981	2.981
C_{rot}	2.981	2.981
C_{vib}	33.818	36.895
C_{tot}	39.780	42.857
Entropy (S) (Cal/mol-K)		
S_{trans}	41.045	41.045
S_{rot}	30.117	30.169
S_{vib}	26.600	30.120
S_{tot}	97.762	101.334

Table 5 — Thermodynamic properties of BTA at different temperatures at B3LYP/6-311+G level

T (Kelvin)	$Є_{tot}$ (Kcal/mol)	C_v (cal/mol-K)	S (Cal/mol-K)	H (Kcal/mol)
293	122.1	42.3	100.6	237.9
303	122.5	43.4	102.1	238.4
313	122.9	44.6	103.5	238.9
323	123.4	45.7	105.0	239.4
333	123.9	46.8	106.5	239.9
343	124.4	47.9	107.9	240.4
353	124.8	49.1	109.4	240.9
363	125.4	50.2	110.9	241.4
373	125.9	51.2	112.3	241.9

The variation in thermodynamic properties at different temperatures has been studied using the B3LYP/6-311+G optimized geometry and it is observed that the thermodynamic function value increases with increase of the temperature (Table 5).

Hence, the variation in thermodynamic properties with temperature can be attributed to the fact that as the temperature increases, the intensities of molecular vibration also increase[13,30]. The correlations between these thermodynamic properties and temperature are shown in Fig. 4. The empirical correlations between the thermodynamic properties and temperature are deduced as follows:

$$H = 0.05\ T + 223.2$$
$$C_v = -4\times10^{-5}\ T^2 + 0.137\ T + 5.21$$
$$E_{tot} = 8\times10^{-5}\ T^2 - 0.003\ T + 116.4$$
$$S = -3\times10^{-6}\ T^2 + 0.148\ T + 57.32 \quad \ldots (2)$$

All the above mentioned thermodynamic data is helpful for the further studies on BTA. As all these thermodynamic calculations have been done in gas phase and can be used to compute the other thermodynamic energies according to the relationship of thermodynamic functions and estimate chemical reaction directions according to the second law of thermodynamics in thermochemistry[31].

7 Non-Linear Optical Properties

The optical properties like total dipole moment (μ_{tot}), mean polarizability (α_m), molecular first hyperpolarizability (β_μ), and total hyperpolarizability (β_{tot}) have been calculated by using B3LYP/6-311+G and HF/6-311+G optimized geometries. The values of all these properties have been calculated using standard equations available in literature[13,32-35].

The total dipole moment can be calculated using the following equation:

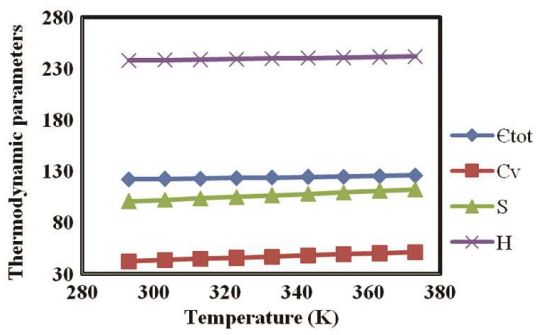

Fig. 4 — Correlation graph between temperature (in Kelvin) and thermodynamic properties like enthalpy (H), Entropy (S), specific heat (C_v) and total energy ($Є_{tot}$) of BTA

$$\mu_{tot} = [(\mu_x^2 + \mu_y^2 + \mu_z^2)]^{1/2} \quad \ldots(3)$$

The mean linear polarizability is defined as:

$$\alpha_m = (1/3)(\alpha_{xx} + \alpha_{yy} + \alpha_{zz}) \quad \ldots(4)$$

The first hyperpolarizability along the dipole moment direction can be given as:

$$\beta_\mu = (3/5)\,[(\beta_x\mu_x + \beta_y\mu_y + \beta_z\mu_z) / |\mu| \quad \ldots(5)$$

Considering Kleinman symmetry[35] in the static limit, the β_x, β_y and β_z can be given as:

$$\begin{aligned}\beta_x &= \beta_{xxx} + \beta_{xyy} + \beta_{xzz}\\ \beta_y &= \beta_{yxx} + \beta_{yyy} + \beta_{yzz}\\ \beta_z &= \beta_{zxx} + \beta_{zyy} + \beta_{zzz}\end{aligned} \quad \ldots(6)$$

The total hyperpolarizability is defined as:

$$\beta_{tot} = [(\beta_x^2 + \beta_y^2 + \beta_z^2)]^{1/2} \quad \ldots(7)$$

The calculated values for the above mentioned parameters in Eqs (3-7) are obtained by a frequency job output from Gaussian software[11] and are shown in Table 6. The calculated dipole moment, polarizability and total hyperpolarizability values of BTA (0.55 Debye, 17.13×10^{-24} esu, 1.17×10^{-30} esu and 2.87×10^{-30} esu, respectively, in B3LYP method and 0.41 Debye, 15.43×10^{-24} esu, and 2.1×10^{-30} esu, respectively, in HF method) are listed in Table 6. Urea is a standard prototypical molecule which is used for the comparison of the NLO properties of molecular systems. And the β-value of the urea molecule was used frequently as a threshold value for the purpose of comparison. Here also the calculated β_{tot} value of BTA is compared with urea, and found to be 9.6 (B3LYP)/7.1(HF) times more than that of urea[36] (0.2991×10^{-30} esu).

Table 6 — The dipole moment (in Debye), polarizability (in esu), hyperpolarizabilities (in esu) tensors computed with the B3LYP/6-311+G and HF/6-311+G methods

	B3LYP/6-311+G	HF/6-311+G		B3LYP/6-311+G	HF/6-311+G
μ_x	0.2770	0.20	β_{xxx}	97.572	32.35
μ_y	-0.0003	-0.00003	β_{xxy}	-0.004	-0.008
μ_z	-0.4750	-0.3500	β_{xyy}	39.8	53.46
μ_{tot}	0.55	0.41	β_{yyy}	-0.006	0.050
			β_{xxz}	49.6	15.3
α_{xx}	134.1	121.3	β_{xyz}	-0.003	-0.018
α_{xy}	0.001	0.006	β_{yyz}	18.12	19.58
α_{yy}	84.7	77.9	β_{xzz}	-40.82	-40.14
α_{xz}	-10.26	-8.41	β_{yzz}	0.003	0.011
α_{yz}	0.0007	0.0050	β_{zzz}	250.25	201.7
α_{zz}	127.97	113.12	β_μ	1.17×10^{-30}	0.95×10^{-30}
α_m	17.132×10^{-24}	15.43×10^{-24}	β_{tot}	2.87×10^{-30}	2.1×10^{-30}

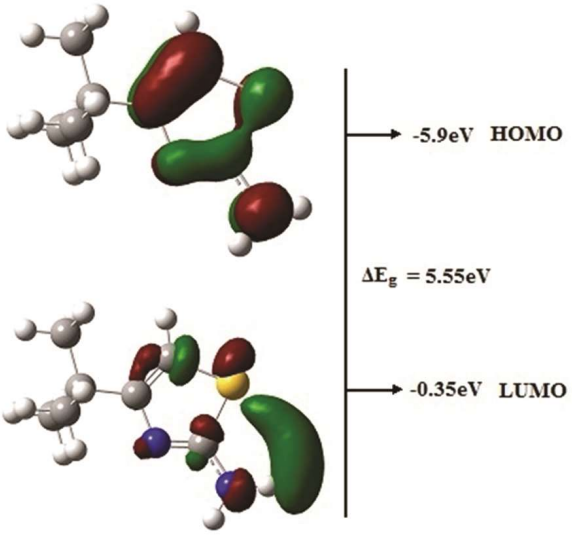

Fig. 5 — Frontier molecular orbitals (HOMO and LUMO) and the energy gap (ΔE_g) of BTA

8 HOMO-LUMO Energy Gap

The study of the frontier molecular orbitals, i.e., highest occupied molecular orbital (HOMO), lowest unoccupied molecular orbital (LUMO) and the HOMO–LUMO energy gap (ΔE_g) energies of an organic molecule are significant in determining the way in which the molecule interacts with other species and also the chemical activity of the molecule[37-40]. The HOMO represents the ability to donate an electron whereas the LUMO represents the ability to obtain an electron. According to the Koopman's theory, the energy of HOMO is related to the ionization potential and LUMO is related to the electron affinity of molecule[39]. The electronic absorption corresponds to the transition from the ground to the first excited state and is mainly described by the excitation of one electron from the HOMO to LUMO. The HOMO, LUMO and ΔE_g energies of the title molecule have been calculated using B3LYP/6-311+G method and the results are shown in Fig. 5. The ΔE_g for BTA has been calculated as 5.55 eV, which is a critical parameter in determining the molecular charge transport property, there by measuring the conductivity of the molecule.

9 Conclusions

In the present study, the structural geometrical parameters, vibrational frequencies, thermodynamic

and nonlinear optical properties of BTA have been studied using both the B3LYP and HF methods with 6-311+G basis set. The structural parameters like bond length and angles obtained are in good agreement with reported values of thiazoles. It can be seen that the calculated vibrational frequencies of BTA computed using DFT/B3LYP/6-311+G method are in good agreement with the experiment. The spectral frequencies have been calculated using both the above mentioned methods and are compared with the observed spectra. The complete vibrational assignments of wavenumbers have been made on the basis of potential energy distribution and found to be in good agreement with the experiment. The differences between the calculated and observed frequencies of N-H vibrations are higher when compared to C-H, C-C, C-N and C-O frequencies. The values of asymmetric and symmetric stretching vibrations of methyl are in good agreement with the experimental values. The thermodynamic properties have been calculated for the title molecule using both the B3LYP and HF method using 6-311+G basis set and may be helpful in the estimation of chemical reaction directions. Using the B3LYP/6-311+G optimized geometry, the thermodynamic properties are calculated at constant pressure by varying the temperature and the correlation between them is found to be linear. The polarizability, first hyperpolarizability, and total hyperpolarizability imply that the title molecule may be useful as a NLO material. Furthermore, from the molecular orbital analysis, it can be seen that there is a possibility of intermolecular charge transfer within the molecule. From these studies, it can be concluded that the theoretical methods are very useful in predicting the geometrical, vibrational, optical, thermodynamic and charge transfer properties for the new molecule in advance.

Acknowledgment

One of the authors V V K, thanks to Dr K Bhanuprakash, Chief Scientist, IICT, for his helpful discussions and also Head of the Department of Physics, Osmania University for his kind cooperation.

References

1 Fontecave M, Ollagnier-de-Choudens & Mulliez E, *Chem Rev*, 103 (2003) 2149.
2 Kleemann A, Engel J, Kutscher B & Reichert D, *Pharmaceutical substances: Syntheses, patents and applications*, 4th Edition, (Stuttgart, Thieme), 2001.
3 Wang L Y, Zhang C X, Liu Z Q & Lio D Z, *Inorg Chem Commun*, 6 (2003) 1255.
4 Al-Dujali A H, Atto A T & Al-Kurde A M, *Eur Poly J*, 37 (2001) 927.
5 Li Y, Xu Y, Qian X & Qu B, *Tetrahedron Lett*, 45 (2004) 1247.
6 Tintcheva I, Maximova V, Deligeorgiev T & Zaneva D, *J Photochem Photobiol A Chem*, 130 (2000) 7.
7 Wang Q, Li H, Li Y & Huang R, *J Agri Food Chem*, 52, (2004) 1918.
8 Yanagimoto K, Lee K G, Ochi H & Shibamoto T, *J Agri Food Chem*, 50 (2002) 5480.
9 Parr R G & Yang W, *Density functional theory of atoms and molecules*, (Oxford University Press), 1989.
10 Kumar P V, Narender M, Sridhar R & Nageswar Y V D, *Synth Commun*, 37 (2007) 4331.
11 Frisch M J, Trucks G W, Schlegel H B, Scuseria G E, Robb M A, Cheeseman J R, Montgomery J A, Vreven T, Kudin K N, Burant J C, Millam J M, Iyengar S S, Tomasi J, Barone V, Mennucci B, Cossi M, Scalmani G, Rega N, Petersson G A, Nakatsuji H, Hada M, Ehara M, Toyota K, Fukuda R, Hasegawa J, Ishida M, Nakajima T, Honda Y, Kitao O, Nakai H, Klene M, Li X, Knox J E, Hratchian H P, Cross J B, Adamo C, Jaramillo J, Gomperts G, Stratmann R E, Yazyev O, Austin A J, Cammi R, Pomelli C, Ochterski J W, Ayala P Y, Morokuma K, Voth G A, Salvador P, Dannenberg J J, Zakrzewski V G, Dapprich S, Daniels A D, Strain M C, Farkas O, Malick D K, Rabuck A D, Raghavachari K, Foresman J B, Ortiz J V, Cui Q, Baboul A G, Clifford S, Cioslowski J, Stefanov B B, Liu G, Liashenko A, Piskorz P, Komaromi I, Martin R L, Fox D J, Keith T, Al-Laham M A, Peng C Y, Nanayakkara A, Challacombe M, Gill P M W, Johnson B, Chen W, Wong M W, Gonzalez C & Pople J A, (Gaussian Inc, Wallingford CT), 2004.
12 Vasantha K V, Goud S L & Laxmikanth R J, *Spectrochim Acta A*, 103 (2013) 304.
13 Vasantha K V, Nagabhushanam M & Laxmikanth R J, *Spectrochim Acta A*, 116 (2013) 31.
14 Pulay P, Zhou X & Fogarasi G, (in: R Fransto (Edn.), 406, Kluwer, Dordrecht), NATO AS Series, 1993.
15 De Mare G R, Panchenko Y N & C W Bock, *J Phys Chem*, 98 (1994) 1416.
16 Yamakita Y & Tasuni M, *J Phys Chem*, 99 (1995) 8524.
17 Rauhut G & Pulay P, *J Phys Chem*, 99 (1995) 3093.
18 Jamroz M H, *Spectrochim Acta Part A: Mol Biomol Spectrosc,* 114 (2013) 220.
19 Frisch M J, Nielsen M B & Holder A J, *Gauss view user's manual* (Gaussian Inc., Pittsburgh, PA), 2000.
20 Nygaard L, Asmussen E & Hog J H , *J Mol Struct,* 8 (1971) 225.
21 Hazra D K, Mukherjee M & Mukherjee A K, *J Mol Struct*, 1039 (2013) 153.
22 Silverstein R M & Webster F X, *Spectrometric identification of organic compounds*, (Wiley, USA), 1998.
23 Bellamy L J, *The infrared spectra of complex molecules*, (Chapman and Hall, London), 1980.
24 Singh P P & Srivastava A K, *Aust J Chem*, 27 (1974) 509.
25 Mijović M P V & Walker J, *J Chem Soc*, (1961) 3381.
26 Rao C N & Venkataraghavan R, *Can J Chem*, 42 (1964) 43.
27 Taurins A, Fenyes J G E & Jones R N, *Can J Chem*, 35 (1965) 423.
28 Sbrana G, Castellucci E & Ginanneschi M, *Spectrochim Acta A*, 23 (1967) 751.

29 Reed A E, Curtiss L A & Weinhold F, *Chem Rev*, 88 (1988) 899.
30 Yazıcı S, Albayrak C & Gumrukcuoglu I E, *Spectrochim Acta A*, 93 (2012) 208.
31 Zhang R, Dub B & Sun G, *Spectrochim Acta A*, 75 (2010) 1115.
32 Cinar M, Ali Coruh & Karabacak M, *Spectrochim Acta A*, 83 (2011) 561.
33 Ben Ahmed A, Feki H, Abid Y & Minot C, *Spectrochim Acta A*, 75 (2010) 1315.
34 Asghari-Khiavi M, Hojati Talemi P & Safinejad F, *J Mol Struc Theochem*, 910 (2009) 56.
35 Kleinman D B, *Phy Rev*, 126 (1962) 1977.
36 Ledoux I & Zyss J, *Chem Phys*, 73 (1982) 203.
37 Fukui K, *Science*, 218 (1982) 747.
38 Kose E, Atac A & Karabacak M, *Spectrochim Acta A*, 75 (2010) 1315.
39 Govindarajan M & Karabacak M, *Spectrochim Acta A*, 114 (2013) 1038.
40 Marshall D & Newton, *J Chem Phys*, 48 (1968) 2825